$HfFeGa_2$ and $HfMnGa_2$: Transition-metal-based itinerant ferromagnets with low Curie temperatures

C. Marques,[1,2] Y. Janssen,[1] M. S. Kim,[1,2] L. Wu,[2] S. X. Chi,[3] J. W. Lynn,[3] and M. C. Aronson[1,2,*]

[1]*Brookhaven National Laboratory, Upton, New York 11973, USA*

[2]*Department of Physics and Astronomy, Stony Brook University, Stony Brook, New York 11794, USA*

[3]*NIST Center for Neutron Research, National Institute of Standards and Technology, 100 Bureau Drive, Gaithersburg, Maryland 20899, USA*

(Received 12 October 2010; revised manuscript received 4 April 2011; published 31 May 2011)

We present a report on the physical properties of the transition-metal-based ferromagnets $HfFeGa_2$ and $HfMnGa_2$. The magnetic susceptibility in both displays Curie-Weiss behavior at high temperature that is replaced by the critical susceptibility just above the Curie temperatures, which are 47.9 K in $HfFeGa_2$ and 25.6 K in $HfMnGa_2$. The ferromagnetically ordered state has a coercive field of 1700 Oe in $HfFeGa_2$ and 320 Oe in $HfMnGa_2$, with strong anisotropy that largely confines the moments to the b axis. Critical exponents that are derived from neutron diffraction measurements and Arrott plot analyses of the magnetization confirm the mean-field character of the ferromagnetic transitions. Phonons dominate the specific heat at all temperatures, but clear ordering anomalies accompany the onset of ferromagnetic order, as well as an electronic component that is larger in the ordered than paramagnetic states. Both $HfFeGa_2$ and $HfMnGa_2$ are metallic, and we observe an anomalous exponent in the temperature-dependent resistivity $\rho(T)$, where $\rho(T) - \rho_0 = BT^{5/3}$, signaling that the ordered state is a marginal Fermi liquid. Overall, the robustness of ferromagnetic order, the Curie temperatures, and the impact of fluctuations in both $HfFeGa_2$ and $HfMnGa_2$ are very similar to those of previously studied ferromagnets, such as MnSi, $ZrZn_2$, Ni_3Al, and Sc_3In.

DOI: 10.1103/PhysRevB.83.184435 PACS number(s): 75.30.Kz, 75.40.−s, 75.50.Cc

I. INTRODUCTION

Metallic ferromagnets have played a central role in the development of theories of magnetic materials, initially establishing that ferromagnetism occurs as a collective Stoner instability of interacting conduction electrons.[1] The Stoner theory can be extended through the incorporation of spin fluctuations,[2–4] which represent the increasing instability of the magnetization as the system is tuned to ever lower Curie temperatures, and ultimately the non-Fermi-liquid-behavior that occurs when ferromagnetic order is completely suppressed. Most recently, interest has focused on systems where ferromagnetic order can be brought to the brink of instability, using pressure, magnetic field, or composition to drive the Curie temperature T_C to zero temperature. Experiments reveal an unexpected richness of behavior in these systems, results that are not yet fully explained in the context of current theory.[5–7] What are the other collective phases that are possible, once magnetic order has been suppressed? What are the properties of the magnetic excitations near such a ferromagnetic instability, and how do they couple to the underlying electronic structure to produce novel phases such as magnetically mediated superconductivity?

Much of what we know about the answers to these intriguing questions comes from experiments conducted on a very limited number of transition-metal-based and ferromagnetic compounds such as MnSi ($T_C = 29.5$ K),[8] $ZrZn_2$ ($T_C \leqslant 28$ K),[9] Sc_3In ($T_C = 6$ K,[10] 7.5 K[11]), and Ni_3Al ($T_C = 42$ K)[12] that have transition temperatures that are low enough that a tuning parameter Γ, which can be pressure, magnetic field, or even composition, can drive $T_C \to 0$, forming a quantum critical point (QCP) at $\Gamma = \Gamma_C$. In the mean-field limit, the Curie temperature T_C for a three-dimensional ferromagnet is suppressed to zero as $T_C \approx (\Gamma - \Gamma_C)^{3/4}$. Normal Fermi-liquid behavior is found deep in the ferromagnetic phase ($\Gamma \ll \Gamma_C$) and also in the paramagnetic phase ($\Gamma \gg \Gamma_C$) at low temperatures, where the electrical resistivity $\rho = \rho_0 + AT^2$, the heat capacity $C \sim \gamma T$, and the magnetic susceptibility $\chi(T) \sim \chi_0$. Marginal Fermi-liquid behavior is predicted in the paramagnetic phases where $\rho(T) \sim \rho_0 + BT^{5/3}$,[13] $C \sim T \ln(T^*/T)$,[14] and $\chi(T)^{-1} \sim \chi_0 + aT^{4/3}$.[2,4,15] These predictions have been tested in several different systems. Essentially complete agreement with each of these predictions is found for $Ni_{1-x}Pd_x$ ($x_C = 0.025$),[16] while studies of the ferromagnet Ni_3Al under pressure[17] similarly found that the electrical resistivity $\rho(T) \sim \rho_0 + BT^{5/3}$. Both doping and pressure have been used to create a ferromagnetic quantum critical point in $ZrZn_2$,[18,19] and in both cases it is found that $T_C \approx (\Gamma - \Gamma_C)^{3/4}$, while near the QCP, $\chi(T)^{-1} \sim \chi_0 + aT^{4/3}$, with χ_0 vanishing, and as well as $\rho(T) \sim \rho_0 + BT^{5/3}$.

As sample quality continues to improve, it has become increasingly evident that the transition from the ordered phase to the paramagnetic phase at the QCP is not universally continuous, but can also have first-order character. This was subsequently shown via field theoretical techniques to be a generic feature of QCPs in clean ferromagnets, although in the presence of strong magnetic fluctuations or with strong disorder, the transition is expected to remain second order.[7] Perhaps the most extensively studied compound is MnSi, where magnetic susceptibility measurements found that the ferromagnetic phase transition is second order for pressures less than 1.2 GPa, becoming weakly first order as the pressure approaches the QC pressure of 1.6 GPa.[20] Similar observations were made in refined crystals of $ZrZn_2$.[21] In both cases, there is substantial evidence for fluctuations accompanying magnetic order in the vicinity of the critical pressure, implying that the phase transition is weakly first order. Nonetheless, a new temperature dependence for the electrical resistivity

$\rho(T) \sim \rho_0 + cT^{3/2}$ was found in the vicinity of the QCP in MnSi,[22] and into the high-pressure paramagnetic phase as well.[23]

Less well understood is the relationship between the unconventional fluctuations associated with the QCP, present even in systems that avoid quantum criticality via a first-order transition, and the stabilization of superconductivity. In part, this is because the most detailed studies of these fluctuations have been carried out on the compounds mentioned above, none of which is superconducting. So far, the only systems where superconductivity emerges from a ferromagnetically ordered phase involving the same electrons are uranium based: UGe_2,[24] URhGe,[25] UIr,[26] and UCoGe.[27]

The interplay of superconductivity and ferromagnetic order, phases that at one time were considered mutually exclusive, has excited great theoretical interest.[28–32] While theory generally agrees with experiments that proximity to a QCP is important for stabilizing unconventional superconductivity, they do not agree on whether special conditions prevail in the uranium based compounds that permit the coexistence of superconductivity and ferromagnetism, or whether the superconductivity has any generic aspects, to be found in virtually any quantum critical ferromagnet of sufficient cleanliness. Second, the impact of the first-order character of the ferromagnetic phase line on superconductivity is still incompletely explored.[33] Key questions such as the symmetry of the order parameter, the nature of the gap, and the spatial texture of the superconducting state are largely unanswered. For all these reasons, there is a pressing need to identify new materials where these issues can be more extensively investigated. Of special significance is to identify a new ferromagnetic superconductor that is not uranium based. We make a step toward fulfilling these needs by exploring the properties of $HfFeGa_2$ and $HfMnGa_2$, which we will show are itinerant ferromagnets. Their low Curie temperatures suggest that they could be pressure tuned to quantum criticality, perhaps revealing superconductivity.

II. EXPERIMENTAL DETAILS

The physical properties of $HfFeGa_2$ and $HfMnGa_2$ have not been reported previously. We present here the results of ac magnetic susceptibility χ' and dc magnetization $M(H)$ measurements, both performed on oriented crystals of $HfFeGa_2$ and $HfMnGa_2$ using a Quantum Design magnetic property measurement system (MPMS). χ' was determined using a 0.4 mT ac field, with a measuring frequency of 17 Hz. The temperature dependencies of the specific heat C and electrical resistivity ρ were obtained using a Quantum Design physical property measurement system (PPMS). ρ was measured in the standard four-probe configuration. For $HfMnGa_2$, the current flowed along the crystallographic a axis, but the direction of the current flow was not along any of the principal crystallographic directions for the $HfFeGa_2$ crystal. Neutron powder diffraction data were collected between 10 and 300 K using the triple-axis spectrometer BT-9 at the NIST Center for Neutron Research (NCNR). A 30 mg single crystal of $HfFeGa_2$ was mounted in a closed-cycle refrigerator and was aligned so that a (301) reflection was in the Bragg condition for the neutrons produced by a PG002 monochromator ($\lambda = 2.36$ Å).

III. EXPERIMENTAL RESULTS

We synthesized single crystals of $HfFeGa_2$ and $HfMnGa_2$ from Ga flux using the ratios (Hf:Fe:Ga = 1:1:20) and (Hf:Mn:Ga = 1:4:5). The $HfFeGa_2$ crystals form as faceted blocks, approximately 1–2 mm on a side, while the $HfMnGa_2$ crystals are rodlike, with typical dimensions of 3 mm long and 1 mm in both of the perpendicular directions. Powder x-ray and neutron diffraction measurements were used to verify the previously reported crystal structures[34] for $HfFeGa_2$ and $HfMnGa_2$.

We confirm that both $HfFeGa_2$ and $HfMnGa_2$ form in the $HfFeGa_2$ oP48 structural prototype, with the *Pnma* space group. The $HfFeGa_2$ structure is shown in Fig. 1, and a summary of the lattice constants and other pertinent atom spacings in $HfFeGa_2$ and $HfMnGa_2$ are presented in Table I.

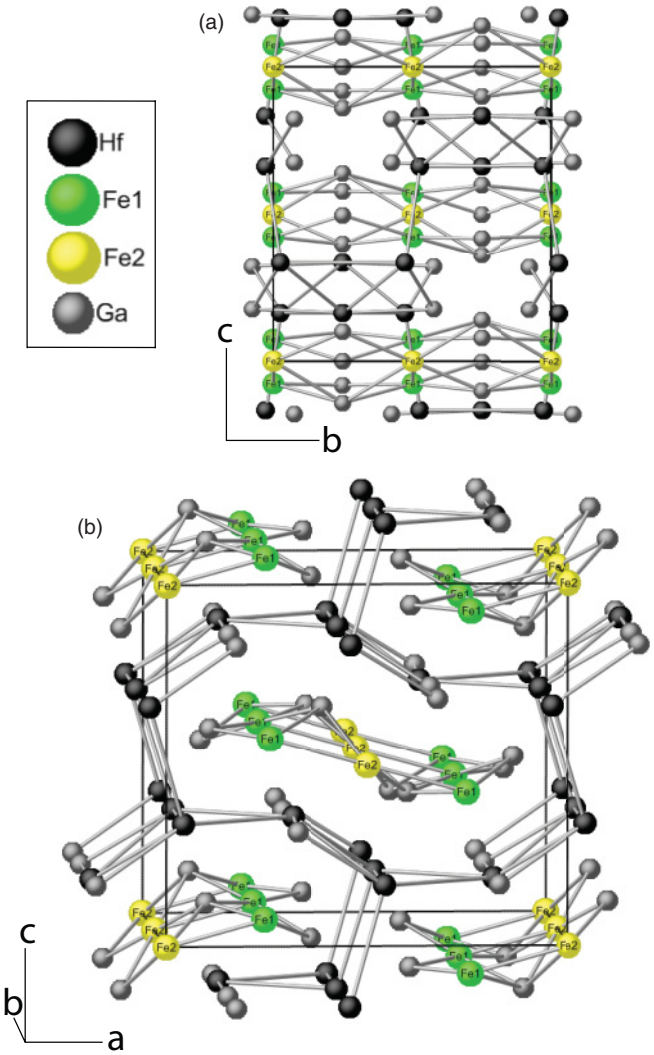

FIG. 1. (Color online) Two different perspective views of a unit cell of $HfMGa_2$ (M = Fe, Mn) (dotted lines), with atom types as indicated in key. (a) The *b*-*c* plane. Note the columns of Fe1 (Mn1) and Fe2 (Mn2) atoms along the *b* axis. (b) The columns of Fe (Mn) atoms are surrounded by a distorted, tubelike cage of Ga atoms. Atomic spacings are not to scale. See Table I for information about atom spacings.

TABLE I. Room-temperature lattice constants and key atom spacings for $HfFeGa_2$ and $HfMnGa_2$, where M1 and M2 are Fe1/Mn1 and Fe2/Mn2, respectively.

	$HfFeGa_2$	$HfMnGa_2$
a (nm)	0.9906	0.9985
b (nm)	0.8415	0.8431
c (nm)	0.8949	0.9003
M1-M1 (interchain) (nm)	0.4475	0.4502
M1-M1 (intrachain) (nm)	0.4223	0.4200
M2-M2 (interchain) (nm)	0.6675	0.6722
M2-M2 (intrachain) (nm)	0.4207	0.4215
M1-M2 (nm)	0.2573	0.2593
M1-Ga (nm)	0.2470	0.2432
M2-Ga (nm)	0.2478	0.2573

There are two inequivalent Fe (Mn) atoms in this structure, and they are arranged in separate columns along the b axis. The closest Fe-Fe distance is between neighboring columns, while the Fe1-Fe1 (Mn1-Mn1) and Fe2-Fe2 (Mn2-Mn2) distances along the columns are identical. The nearest neighbors of the Fe (Mn) atoms are Ga atoms, which form cagelike channels that surround the isolated Fe1 (Mn1) and Fe2 (Mn2) columns. Single-crystal x-ray diffraction measurements were used to index the facets of $HfFeGa_2$ and $HfMnGa_2$, where the a axis was found to be along the rod axis. The nominal structures of $HfFeGa_2$ and $HfMnGa_2$ were also confirmed using single-crystal x-ray diffraction measurements. Although strong absorption from Hf limited the accuracy of our fits, we obtained a refinement factor $R1 = 0.0164$, permitting no more than 1%–2% variation in site occupancy.

The magnetic characters of $HfFeGa_2$ and $HfMnGa_2$ are evident from their ac magnetic susceptibilities χ', plotted in Fig. 2. In both cases, χ' can be described by a Curie-Weiss law for temperatures between ≈100–300 K for $HfFeGa_2$ and ≈60–300 K in $HfMnGa_2$ [Figs. 2(c) and 2(d)]. The moments deduced from these fits are $2.3 \pm 0.1\ \mu_B$/Fe and $1.6 \pm 0.1\ \mu_B$/Mn, while $HfFeGa_2$ has a Weiss temperature $\theta = 60 \pm 2$ K, and $\theta = 28 \pm 2$ K for $HfMnGa_2$. Figures 2(a) and 2(b) show that there is virtually no anisotropy in χ' for either compound over the range of temperatures where the Curie-Weiss laws are observed. A large and very sharp peak is observed at 47.9 K in $HfFeGa_2$ and at 25.6 K in $HfMnGa_2$, signaling the onset of magnetic order. There is substantial magnetic anisotropy in the magnetically ordered state, where the extrapolated $T \to 0$ values for χ' are ≈10 times smaller in both $HfFeGa_2$ and $HfMnGa_2$ when the field is along the b axis, than when it is along either a or c. The insets of Figs. 2(a) and 2(b) show expanded views of χ', demonstrating that additional peaks are present for $HfFeGa_2$ and $HfMnGa_2$ above the main ordering peak when $B \| b$. These peaks appeared in all samples with similar relative strengths and are insensitive to the field orientation, but are absent in the dc magnetization measurements, which are carried out in fields larger than 1 T. One possibility is that Fe1 (Mn1) and Fe2 (Mn2) sites order separately, at slightly different temperatures. Alternatively, small deviations in composition or site occupancy consistent with our refinement of the single-crystal x-ray diffraction measurements may result in the formation of secondary

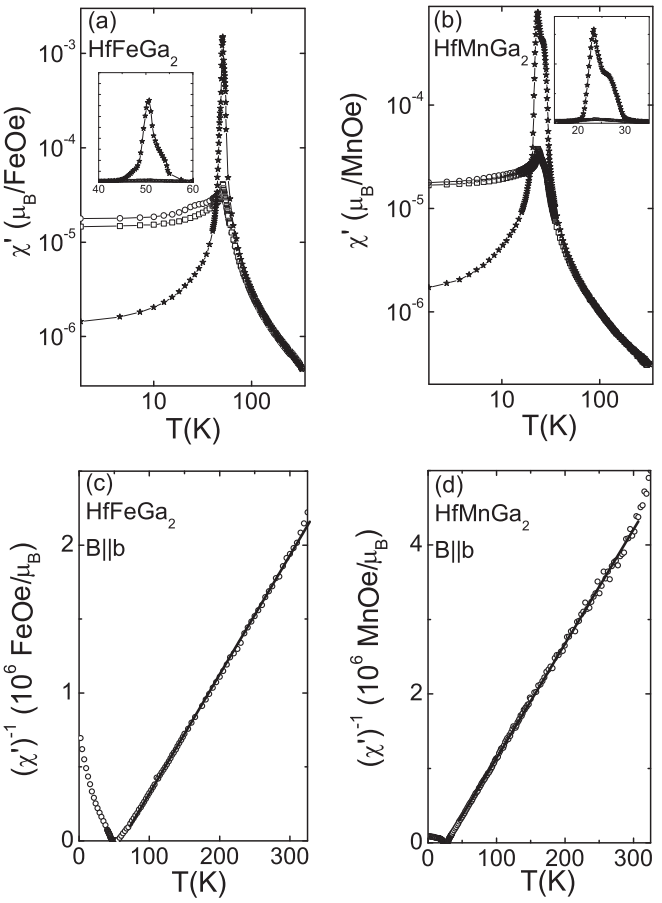

FIG. 2. The temperature dependencies of the ac magnetic susceptibility χ' for $HfFeGa_2$ (a) and $HfMnGa_2$ (b), for the 0.4 mT field in all three crystallographic directions, $B \| a$ (□), $B \| b$ (∗), and $B \| c$ (○). Insets show expanded views of temperatures near the ordering temperatures. The temperature dependencies of the inverses of the ac magnetic susceptibilities $(\chi')^{-1}$ for $HfFeGa_2$ (c) and $HfMnGa_2$ (d) with $B \| b$ demonstrate Curie-Weiss behaviors at high temperatures (solid lines). The susceptibility of the sample holder has been subtracted for both $HfFeGa_2$ and $HfMnGa_2$.

ferromagnetic phases that can be saturated in 1 T. Further measurements using more sophisticated probes such as nuclear magnetic resonance or neutron diffraction are required to test these possibilities.

Measurements of the field dependencies of the dc magnetization $M(H)$, presented in Figs. 3(a) and 3(b), confirm that both $HfFeGa_2$ and $HfMnGa_2$ order ferromagnetically at low temperatures. At 1.8 K, $M(H)$ is highly nonlinear, especially for $B \| b$. The approach to saturation is very rapid for $B \| b$, but is much more gradual for fields in the basal plane, reaching saturation moments of ≈0.7 μ_B/Fe in $HfFeGa_2$ and 0.35 μ_B/Mn in $HfMnGa_2$. The saturation moments for $HfFeGa_2$ and $HfMnGa_2$ were confirmed in measurements on two crystals of each compound taken from different batches. Full magnetization loops were measured at 1.8 K, and are presented in Figs. 4(a) and 4(b), clearly demonstrating that the ordered states are ferromagnetic.The loops are symmetrical but not entirely square, and are superimposed on an additional paramagnetic component that increases linearly with increasing field. A coercive field H_c of 1700 Oe is found in

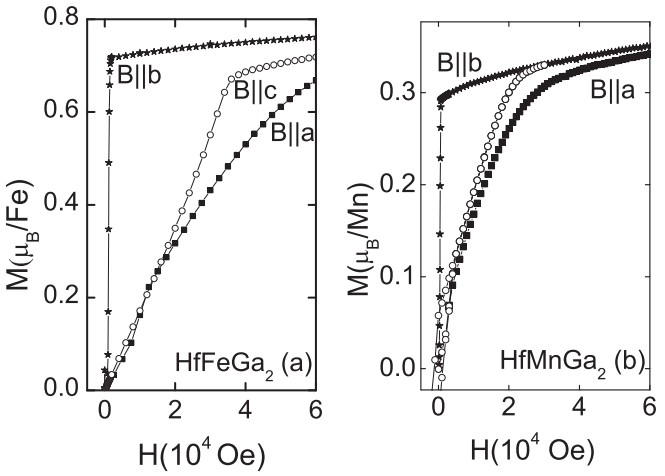

FIG. 3. The field dependencies of the dc magnetization M for $HfFeGa_2$ (a) and $HfMnGa_2$ (b) at 1.8 K, for the dc field in all three crystallographic directions, $B\|a$ (■), $B\|b$ (⋆), and $B\|c$ (○).

$HfFeGa_2$ but is only 320 Oe for $HfMnGa_2$. H_c varies by less than 1%–2% among crystals of both $HfFeGa_2$ and $HfMnGa_2$ taken from different batches.

The field dependencies of the dc magnetization $M(H)$ of $HfFeGa_2$ and $HfMnGa_2$ were measured for a variety of temperatures both above and below their ordering temperatures T_C [Figs. 5(a) and 5(b)], with the aim of obtaining further information about the ferromagnetic phase transitions via Arrott plot analyses. The isotherms of $M(H)$ with $B \geqslant 4$ T are parallel and evenly spaced in the modified Arrott plots ($M^{1/\beta}$ as functions of B/M) presented in Figs. 5(c) and 5(d). We identify $T_C = 47.9$ K as the critical isotherm for $HfFeGa_2$ and 25.6 K for $HfMnGa_2$ [Figs. 5(b) and 5(e)], where we find that $M \propto H^{1/\delta}$, with $\delta = 2.8 \pm 0.1$ for $HfFeGa_2$ [Fig. 5(e)] and 3.7 ± 0.1 for $HfMnGa_2$ [Fig. 5(f)]. The temperature dependence of the spontaneous moment $M_0(T)$ can be determined from the Arrott plots by extrapolating $M^{1/\beta}(T)$ to its value as $B/M \to 0$. $M_0(T)$ is plotted in Fig. 6(a), displaying an order-parameter-like temperature dependence in both $HfFeGa_2$ and $HfMnGa_2$, becoming nonzero at their respective values of T_C and rising to a $T \to 0$ value of 0.5 μ_B/Fe in $HfFeGa_2$ and 0.3 μ_B/Mn in $HfMnGa_2$. Figure 6(b) shows that $M_0 \sim t^\beta$, over a range of reduced temperature $t = (T_C - T)/T_C$ that approaches three orders of magnitude in $HfFeGa_2$ and slightly less in $HfMnGa_2$, giving $\beta = 0.36 \pm 0.02$ in the former and $\beta = 0.37 \pm 0.03$ in the latter. These values for β are not

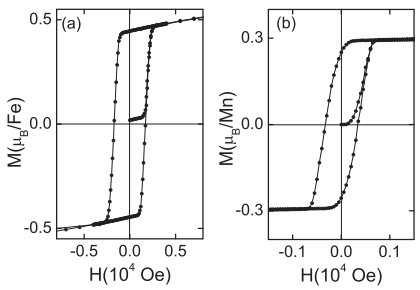

FIG. 4. The full magnetization loops $M(H)$ at 1.8 K with $B\|b$ axis for $HfFeGa_2$ (a) and $HfMnGa_2$ (b).

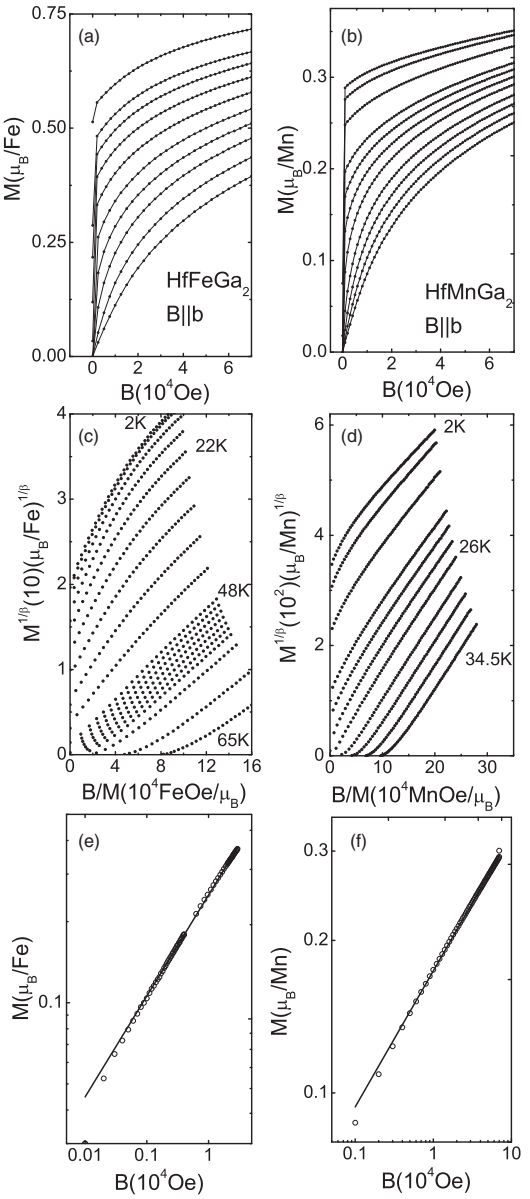

FIG. 5. The field dependencies of the dc magnetization of $HfFeGa_2$ ($B\|b$) (a) and $HfMnGa_2$ ($B\|b$) (b) at different temperatures from 2 K to 65 K. (c) and (d) Modified Arrott plots $M^{1/\beta}$ vs B/M of the same data as (a) and (b), for different isotherms bracketing the critical isotherms. The field dependence of the magnetization $M(H)$ at the critical isotherm, $HfFeGa_2$ in (e), $HfMnGa_2$ in (f). Solid lines indicate power-law fit $M(T_C) \approx H^{1/\delta}$.

consistent with the ferromagnetic transitions being mean-field like, which would give $\beta = 0.5$. However, they are consistent with either Heisenberg ($\beta = 0.333$) or Ising ($\beta = 0.327$) class exponents.

We have confirmed the ferromagnetic order parameter $M_0(T)$ using neutron diffraction measurements. These experiments were carried out on a 30 mg single crystal of $HfFeGa_2$ using the BT-9 triple-axis spectrometer. The temperature-dependent intensity of the magnetic part of the (301) Bragg peak has been scaled to match the $T \to 0$ value of the spontaneous moment $M_0(T)$, and the two measurements are compared in Fig. 6(a). There is excellent agreement between

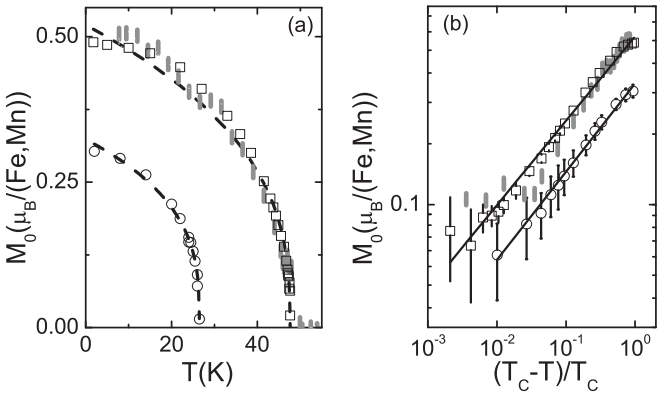

FIG. 6. (a) The temperature dependencies of the spontaneous moment M_0 determined from the Arrott plot analysis in HfFeGa$_2$ (□, $B\|b$) and HfMnGa$_2$ (◯, $B\|c$). The solid gray vertical markers correspond to the temperature-dependent part of the (301) neutron diffraction peak of HfFeGa$_2$, scaled to correspond to the extrapolated $T \to 0$ value of M_0 taken from magnetization measurements. Dashed lines indicate power-law fits, assuming $T_C = 47.9$ K (HfFeGa$_2$) and 25.6 K (HfMnGa$_2$). (b) M_0 as a function of the reduced temperature $t = (T_C - T)/T_C$ for HfFeGa$_2$ (□) and HfMnGa$_2$ (◯). The critical exponent β is taken from the slopes of the solid lines, which are the best power-law fits to the spontaneous moment taken from the Arrott plot analyses. Neutron diffraction intensities (gray vertical lines) are shown for comparison.

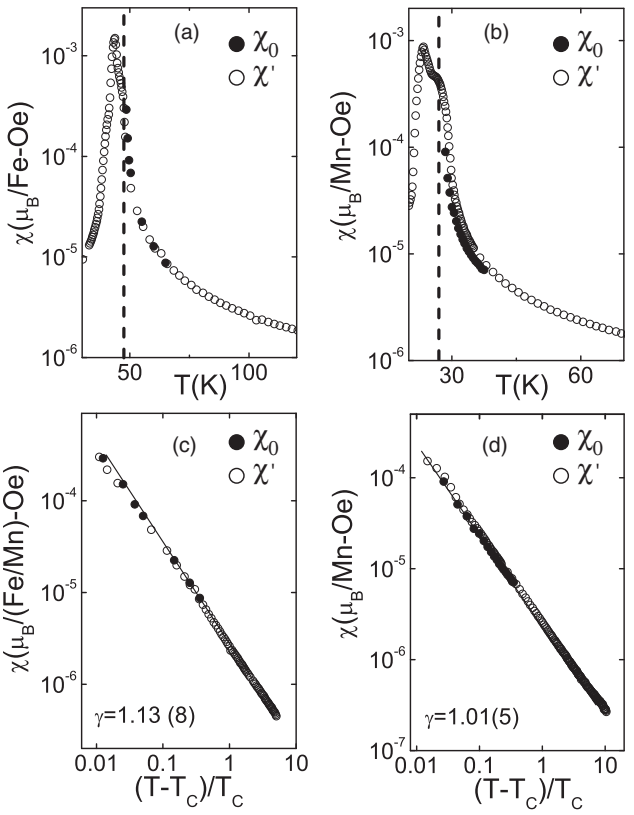

FIG. 7. The temperature dependencies of the initial susceptibility χ_0(●) from the Arrott plot analysis and the real part of the ac susceptibility χ' (◯) for HfFeGa$_2$ (a) and HfMnGa$_2$ (b). Solid lines are guides for the eye, and dashed lines indicate Curie temperatures taken from the maxima in χ'. (c) and (d) Same data plotted as functions of the reduced temperature $t = (T - T_C)/T_C$. Solid lines are best power-law fits to the data, giving slopes $\gamma = 1.13 \pm 0.08$ for HfFeGa$_2$ (c) and $\gamma = 1.01 \pm 0.05$ for HfMnGa$_2$ (d).

these two independent measurements of the HfFeGa$_2$ order parameter, confirming that ferromagnetic order occurs at 47.9 K in HfFeGa$_2$. We note that there is no additional structure in $M_0(T)$ above T_C, where the second peak in the ac susceptibility is observed. Additional experiments in different planes in reciprocal space would be required to definitively rule out the possibility mentioned above of an intrinsically two-step ferromagnetic transition.

While the ac susceptibility χ' is well described by a Curie Weiss law for $T \geqslant 100$ K, a critical response is found in the vicinity of the ferromagnetic transition. χ' is compared in Figs. 7(a) and 7(b) to the initial susceptibility χ_0, taken from the horizontal intercepts of the Arrott plot isotherms. The two measurements are identical in both HfFeGa$_2$ and HfMnGa$_2$, within our experimental accuracy. Figures 7(c) and 7(d) demonstrate that both compounds have power-law temperature dependencies $\chi' = \chi_0 \sim t^{-\gamma}$, with slightly different values of $\gamma = 1.13 \pm 0.08$ in HfFeGa$_2$ and 1.01 ± 0.05 in HfMnGa$_2$.

We have measured the specific heat of a 7.5 mg single crystal of HfFeGa$_2$ and a 12.5 mg single crystal of HfMnGa$_2$ for temperatures 1.8–300 K. The measured specific heat C is broad and featureless in both compounds [Figs. 8(a) and 8(b)]. We have used the Debye model to estimate the specific-heat contribution from the phonons, $C_{\rm ph}$, which we take to be identical in HfFeGa$_2$ and HfMnGa$_2$, with $\theta_D = 314$ K. The high-temperature data of HfFeGa$_2$ [Fig. 8(a)] are well described by the Debye model. We have plotted in Fig. 8(c) the difference between the measured specific heats C for HfFeGa$_2$ and HfMnGa$_2$, divided by temperature, to emphasize that the two measurements differ above 100 K only by a constant that has a magnitude of 0.033 J/mol K^2. We conclude that there is little specific heat in HfFeGa$_2$ above ≈100 K, beyond that originating with the phonons, while HfMnGa$_2$ has an additional electronic specific heat in its paramagnetic state. The combination of the Debye and the electronic contributions describes the measured specific heat of HfMnGa$_2$ very well above ≈100 K [Fig. 8(b)]. Figure 8(c) shows that there is an increasing difference between the specific heats for HfFeGa$_2$ and HfMnGa$_2$ below ≈100 K. Small anomalies are clearly shown at the 47.9 K and 25.6 K ordering temperatures of HfFeGa$_2$ and HfMnGa$_2$, indicated by the dotted vertical lines. We have plotted C/T^3 as a function of temperature in Fig. 8(d) to emphasize that both HfFeGa$_2$ and HfMnGa$_2$ depart from the Debye model of the specific heat below ≈100 K. Both HfFeGa$_2$ and HfMnGa$_2$ show an additional broad shoulder in C/T^3 between ≈10–50 K, which is almost identical in the two compounds. Given the very different Curie temperatures in the two compounds, we conclude that this feature has no direct relationship to critical fluctuations associated with the onset of ferromagnetic order. Similarly, we feel that an explanation in terms of a Schottky anomaly is unlikely, not only because of the delocalized characters of the moments in HfFeGa$_2$ and HfMnGa$_2$, but also because this explanation would require the low-lying states in the putative crystal field and spin orbit split manifolds of the Fe and Mn ions to coincidentally have the same relative

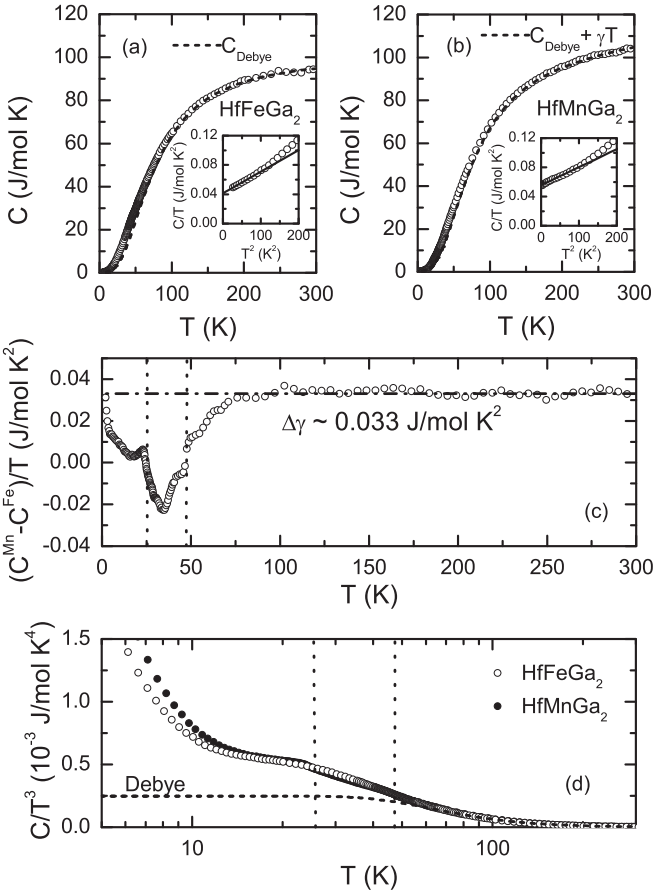

FIG. 8. (a) The measured specific heat of $HfFeGa_2$ (◯). Dashed line shows best fit to Debye model. Inset: C/T vs T^2 plot, demonstrating the $T \to 0$ Sommerfeld constant $\gamma = C/T$. (b) The measured specific heat of $HfMnGa_2$ (◯). Dashed line shows best fit to Debye model plus a term linear in temperature γT (see text). Inset: C/T vs T^2 plot, demonstrating the $T \to 0$ Sommerfeld constant $\gamma = C/T$. (c) The difference between the measured C/T for $HfMnGa_2$ and $HfFeGa_2$. Vertical dotted lines indicate the Curie temperatures of $HfFeGa_2$ (47.9 K) and $HfMnGa_2$ (25.6 K). (d) The measured C/T^3, plotted as a function of T for $HfFeGa_2$ (◯) and $HfMnGa_2$ (●). Vertical dotted lines indicate respective Curie temperatures, while the dashed line indicates the Debye contribution to C/T^3.

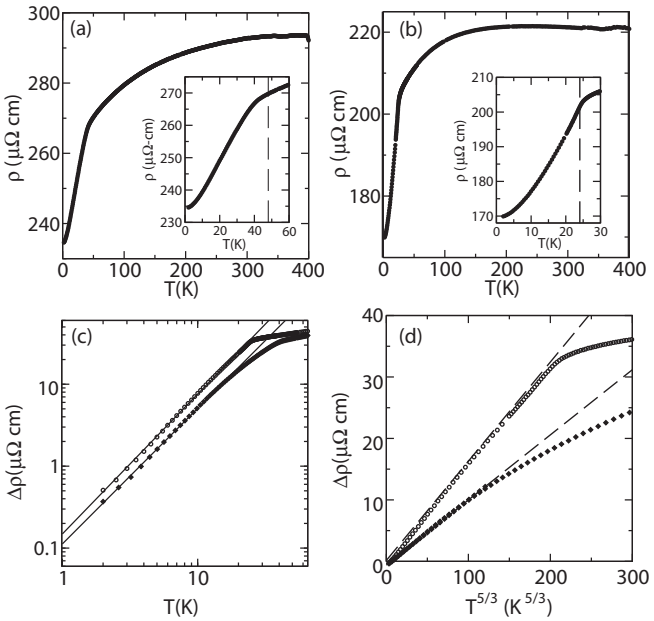

FIG. 9. The temperature dependencies of the resistivity $\rho(T)$ of $HfFeGa_2$ (a) and $HfMnGa_2$ (b). Insets show an expanded view of $\rho(T)$ at low temperatures, where the vertical dashed lines indicate the Curie temperatures taken from ac susceptibility measurements. (c) The resistivity in the ordered state obeys a power law $\Delta\rho = \rho - \rho_0 = AT^n$ in both $HfFeGa_2$ (◆, $n = 1.67 \pm 0.015$) and $HfMnGa_2$ (◯, $n = 1.71 \pm 0.01$) (d). $\Delta\rho$ plotted as a function of $T^{5/3}$. Dashed lines are straight-line fits that show that this temperature dependence persists up to $T_C \approx 25.6$ K in $HfMnGa_2$ (◯) and to ≈18 K in $HfFeGa_2$ (◆).

degeneracies and level spacings. The most likely explanation is that there are low-lying and energetically isolated lattice modes present in both compounds. The cagelike configuration that surrounds the chains of Fe and Mn atoms in the $HfFeGa_2$ and $HfMnGa_2$ structure (Fig. 1) makes an analogy to the skutterudite RT_4Sb_{12} (R = rare earth, T = transition metal) structure appealing, where just such a mode has been observed and is attributed to a "rattling" of the R atoms in the T_4Sb_{12} cage.[35] Unfortunately, attempts to model the broad specific-heat features in $HfFeGa_2$ and $HfMnGa_2$ as isolated Einstein modes were unsuccessful, since they are too broad in temperature to be explained as single Einstein modes. The lattice symmetry does not rule out the possibility of multiple Einstein modes. Finally, we point out that both $HfFeGa_2$ and $HfMnGa_2$ have a considerable electronic specific heat γT as $T \to 0$, where $\gamma = 41$ mJ/mol K^2 in $HfFeGa_2$ and 56 mJ/mol K^2 in $HfMnGa_2$ [insets, Figs. 8(a) and 8(b)]. Since values for γ above T_C are ≈0 for $HfFeGa_2$ and 33 mJ/mol K^2 for $HfMnGa_2$, this implies that the formation of spin-split bands at the onset of ferromagnetic order results in stronger electronic correlations and overall larger electronic masses for both compounds.

Measurements of the temperature dependencies of the electrical resistivities $\rho(T)$ establish $HfFeGa_2$ and $HfMnGa_2$ as metallic compounds [Fig. 9(a) and 9(b)]. In both compounds, $\rho(T)$ decreases monotonically below room temperature, and the onset of ferromagnetic order at T_C is marked by slope discontinuities [insets, Figs. 9(a) and 9(b)]. The residual resistivity ρ_0 is quite large, amounting to 234 $\mu\Omega$ cm in $HfFeGa_2$ and 169 $\mu\Omega$ cm in $HfMnGa_2$, indicating that a substantial degree of disorder is present in both compounds. The temperature-dependent part of the resistivity $\Delta\rho = \rho - \rho_0$ is plotted for both compounds in a double log plot in Fig. 9(c), demonstrating that they follow a power law $\Delta\rho = AT^n$, where $n = 1.67 \pm 0.015$ in $HfFeGa_2$ and $n = 1.71 \pm 0.01$ in $HfMnGa_2$. The power n that is found in these analyses is close to 5/3 in both compounds, and we have plotted $\Delta\rho$ as functions of $T^{5/3}$ in Fig. 9(d) for $HfFeGa_2$ and $HfMnGa_2$ to show that this power law persists virtually to the Curie temperature $T_C = 25.6$ K in $HfMnGa_2$, where the current flows along the a axis, but over a more limited range of temperatures $T \leqslant 18\,\text{K} \approx 0.38T_C$ in $HfFeGa_2$, where the relationship between the current direction and the crystalline axes is not controlled. The power law found in our resistance measurements definitively rules out the possibility that the ferromagnetically ordered

phase is a conventional Fermi liquid with $n = 2$, but instead shows the temperature dependence expected for a marginal Fermi liquid, $n = 5/3$.[4,13]

IV. DISCUSSION

The major finding of this work is the discovery that $HfFeGa_2$ and $HfMnGa_2$ are two new additions to the class of metallic and itinerant ferromagnets with low Curie temperatures, which are 47.9 K for $HfFeGa_2$ and 25.6 K for $HfMnGa_2$. Both compounds have substantial coercive fields of 1700 Oe in $HfFeGa_2$ and 320 Oe in $HfMnGa_2$, as well as strong uniaxial anisotropy in the ordered state, where the crystallographic b axis is the easy magnetic axis. The critical phenomena associated with the onset of ferromagnetic order in $HfFeGa_2$ and $HfMnGa_2$ reveal conventional second-order phase transitions in both. A full set of critical exponents has been determined from the Arrott plot analyses, yielding $\beta = 0.36 \pm 0.02$ in $HfFeGa_2$ (0.37 ± 0.01 in $HfMnGa_2$), $\gamma = 1.13 \pm 0.08$ in $HfFeGa_2$ (1.01 ± 0.05 in $HfMnGa_2$), and $\delta = 2.8 \pm 0.1$ in $HfFeGa_2$ (3.7 ± 0.1 in $HfMnGa_2$). These exponents are compared in Table II to those found in a number of different types of metallic ferromagnets, and with the values expected for the mean field and the three-dimensional Ising and Heisenberg models. The values of γ and δ are in good agreement with the mean-field exponents $\beta = 0.5$, $\gamma = 1$, and $\delta = 3$, but the exponent β is more consistent with either Ising or Heisenberg exponents. In particular, there is no indication in any of these compounds of criticality associated with a nearby quantum critical point, which in mean field would give a contribution to the susceptibility $1/\chi \approx T^{4/3}$.[2,4,15] The general success of this analysis of the critical phenomena similarly demonstrates that the ferromagnetic transitions in $HfFeGa_2$ and $HfMnGa_2$ are decidedly second order, with no evidence for the first-order character that is observed in systems such as MnSi[20] and $ZrZn_2$[21] when pressure reduces their Curie temperatures to ≈0.3–0.5 of their ambient pressure values.

TABLE II. A comparison of the critical exponents found in a variety of metallic ferromagnets with different Curie temperatures T_C to values from different critical models of ferromagnets. β is determined from the spontaneous moment, $M_0 \propto (T_C - T)^{\beta}$, γ from the initial susceptibility $\chi_0 \propto (T - T_C)^{-\gamma}$, and for the critical isotherm, $M \propto H^{1/\delta}$.

Compound	T_C (K)	β	γ	δ	Reference
$HfFeGa_2$	47.9	0.36(2)	1.13(8)	2.8(1)	This work
$HfMnGa_2$	25.6	0.37(3)	1.01(5)	3.7(1)	This work
Ni	635.5	0.399	1.342	4.40	Ref. 36
$SrRuO_3$	150	0.34	1.17		Ref. 37
Ni_3Al	56.38	0.48	0.99 – 1.085	2.998 5	Ref. 38
EuB_6	12.6	0.36	0.88		Ref. 39
$FeNi_3$	872.9	0.4	1.301		Ref. 40
$URu_{1.8}Re_{0.2}Si_2$	0	0.8	0.18	1.23	Ref. 41
Mean field		0.5	1.0	3.0	
3D Heisenberg		0.365	1.387	4.803	Refs. 42,43
3D Ising		0.326	1.237	4.77	Ref. 44
3D FM QCP	0	2	1	1.5	Ref. 7

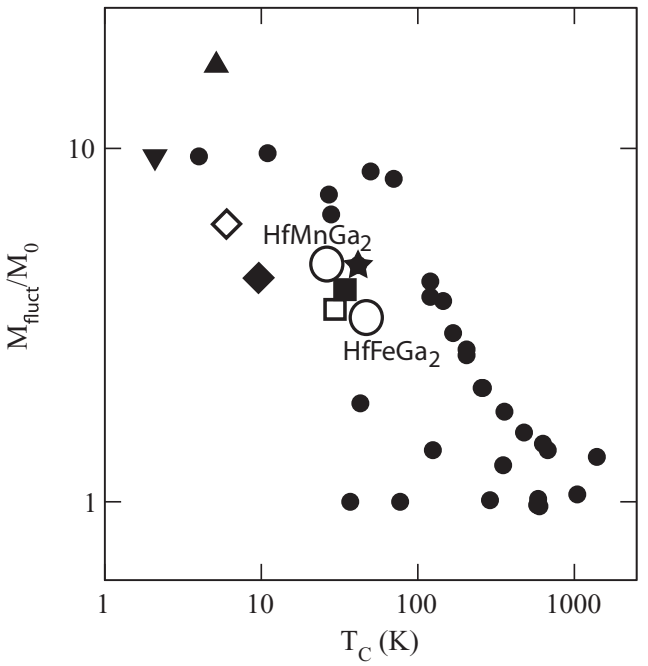

FIG. 10. The Rhodes-Wohlfarth plot of the ratio of fluctuating to static moments in the ordered state of different metallic ferromagnets as a function of their Curie temperatures T_C. $HfFeGa_2$ and $HfMnGa_2$: ◯; MnSi: □ (Ref. 46); $ZrZn_2$: ■ (Ref. 9); Sc_3In: ◇ (Refs. 10,11); URhGe: ◆ (Ref. 52); Ni_3Al: ★ (Ref. 53); UIr_2Zn_{20}: ▼ (Ref. 54); $URh_{1.4}Re_{0.6}Si_2$: ▲ (Ref. 55). Remaining data are from Refs. 45,54.

Critical fluctuations play a decisive role over a wide range of temperatures above and below T_C in $HfFeGa_2$ and $HfMnGa_2$.

$HfFeGa_2$ and $HfMnGa_2$ are in many respects very similar to other itinerant ferromagnets with low Curie temperatures. Ferromagnetism develops from a high-temperature paramagnetic state where the fluctuating moments M_{fluct} taken from Curie-Weiss susceptibilities are consistent with free ion values, i.e., 2.3 μ_B/Fe in $HfFeGa_2$ and 1.6 μ_B/Mn in $HfMnGa_2$. However, the $T = 0$ spontaneous moments M_0 determined from Arrott plot analyses of the magnetization are much smaller, 0.5 μ_B/ Fe in $HfFeGa_2$ and 0.3 μ_B/Mn in $HfMnGa_2$. This implies that relatively little of the moment is static in the ordered state, and the strength of these fluctuations suggests that both $HfFeGa_2$ and $HfMnGa_2$ show signs of impending ferromagnetic instability. To place this result in context, we have plotted the ratio M_{fluct}/M_0 as a function of Curie temperature for a number of metallic ferromagnets in a Rhodes-Wohlfarth plot[45] (Fig. 10), demonstrating the general trend that this ratio becomes larger when ferromagnetic order is restricted to progressively lower temperatures.

$HfFeGa_2$ and $HfMnGa_2$ lie in the same region of the Rhodes-Wohlfarth plot as other stoichiometric, transition-metal-based ferromagnets with similar Curie temperatures, such as MnSi, $ZrZn_2$, Sc_3In, and Ni_3Al. In particular, $HfMnGa_2$ and MnSi are especially well matched, with Curie temperatures of 29.5 K for MnSi[8] and 25.6 K for $HfMnGa_2$, a spontaneous moment of 0.4 μ_B/Mn for MnSi[46] and 0.3 μ_B/Mn for $HfMnGa_2$, and $M_{fluct}/M_0 = 3.5$ for MnSi[46] and 4.85 for $HfMnGa_2$. From this viewpoint, $HfMnGa_2$, and to

a lesser extent $HfFeGa_2$, may be excellent candidates for experiments that would use high pressures to drive $T_C \to 0$, with the aim of revealing non-Fermi-liquid-properties, a bona fide quantum critical point where $T_C \to 0$, or perhaps the crossover to first-order character that was found in MnSi[20,22] and also in $ZrZn_2$.[21]

The properties of the ordered states are also quite similar to those of known metallic ferromagnets. We find values for the Sommerfeld coefficient of the specific heat $\gamma \approx$ 40–60 mJ/mol K^2 that are large in an absolute sense for a transition-metal-based intermetallic compound, but similar to the 36 mJ/mol K^2 found in MnSi[47] and 45 mJ/mol K^2 of $ZrZn_2$.[48] De Haas–van Alphen studies of $ZrZn_2$[49] and MnSi[50] explicitly confirm that the masses of the quasiparticles in the ferromagnetically ordered state are strongly enhanced, relative to their putative values in the noninteracting electronic structure. Ordinarily, the ferromagnetically ordered state is expected to be a Fermi liquid at the lowest temperatures, with $\Delta\rho = \rho(T) - \rho_0 = AT^2$. Instead, we find that $\Delta\rho = BT^{5/3}$ in $HfMnGa_2$ for $T \leqslant T_C$, and for $T \leqslant 0.35T_C$ in $HfFeGa_2$. The large residual resistivities of these compounds prevent us from extending the measurements of $\rho(T)$ to lower temperatures, where a crossover to Fermi-liquid behavior as $T \to 0$ is expected. $\Delta\rho = BT^{5/3}$ is the expected temperature dependence of a marginal Fermi liquid (MFL), where long-ranged magnetic interactions lead to scattering that reduces the quasiparticle lifetime, ultimately to zero as $T \to 0$.[4,13] The distinctive $\Delta\rho = BT^{5/3}$ behavior has been observed in several ferromagnetic systems with low Curie temperatures, suggesting that the magnetic fluctuations found near ferromagnetic QCPs may provide the exact conditions needed to realize the MFL. Previous to our work, $\Delta\rho = BT^{5/3}$ has been observed below a characteristic temperature scale T_{MFL} in three different scenarios involving ferromagnets. First, it is found in $Pd_{1-x}Ni_x$[16] over a wide range of temperatures $0 \leqslant T \leqslant T_{MFL}$, but only at the critical value x_C required to drive T_C to zero. In ambient-pressure $ZrZn_2$, Fermi-liquid behavior is found at the lowest temperatures $T \leqslant T_{FL}$, but $\Delta\rho = BT^{5/3}$ for a wide range of temperatures both above and below T_C, i.e., for $T_{FL} \leqslant T \leqslant T_{MFL}$, where $T_{FL} \leqslant T_C \leqslant T_{MFL}$.[51] Finally, in ambient-pressure Ni_3Al, it is only observed for a range of temperatures $T_{FL} \leqslant T \leqslant T_{MFL}$ deep within the ferromagnetic state, where $T_{MFL} \ll T_C$.[17] Our measurements are consistent with this third scenario in both $HfFeGa_2$, where $T_{MFL} \approx 0.38T_C$ and in $HfMnGa_2$, where $T_{MFL} \approx T_C$. As in most of these previous works, we do not find signatures in $HfFeGa_2$ or $HfMnGa_2$ of the MFL in other measured quantities, such as the specific heat obeying $C/T \propto -\ln T$[4,14] or the temperature-dependent part of the magnetic susceptibility $\chi(T)$ having $[\chi(T) - \chi_0]^{-1} = aT^{4/3}$.[2,4] We speculate that the strong critical susceptibility and the broad phonon peak in the specific heat overwhelm these more delicate signatures of the marginal Fermi liquid that is evidenced by the electrical resistivity.

The observation of MFL behavior in $HfFeGa_2$ and $HfMnGa_2$ is perhaps surprising, since their residual resistivities are as much as several orders of magnitude larger than those found in other MFL systems such as $ZrZn_2$ and Ni_3Al, where disorder can be expected to play a much more limited role. Still, we find MFL behavior over a similarly large range of temperatures in $HfFeGa_2$ and $HfMnGa_2$, and in the former case this behavior extends up to the Curie temperature itself. It is intriguing to note that the MFL signatures in the resistivity of $ZrZn_2$ are most pronounced in the vicinity of the first-order transition produced by high pressures,[51] where the coexistence of ordered and paramagnetic domains can be expected to introduce a new, shorter length scale. It will be interesting to see whether the range of temperatures on which the MFL resistivity $\Delta\rho = BT^{5/3}$ is observed will increase or decrease as we continue to improve the quality of these new itinerant ferromagnets.

ACKNOWLEDGMENTS

This work was carried out under the auspices of the US Department of Energy, Office of Basic Energy Sciences, under Contract No. DE-AC02-98CH1886.

*maronson@bnl.gov

[1] E. C. Stoner, Proc. R. Soc. London A **165**, 372 (1938).
[2] T. Moriya, *Spin Fluctuations in Itinerant Electron Magnetism*(Springer-Verlag, New York, 1985).
[3] G. G. Lonzarich and L. Taillefer, J. Phys. C **18**, 4339 (1985).
[4] G. G. Lonzarich in *Electron*, ed. M. Springford (Cambridge University Press, Cambridge, 1997).
[5] H. von Löhneysen and P. Wölfle, AIP Conf. Proc. **1014**, 107 (2008).
[6] H. von Löhneysen, A. Rosch, M. Vojta, and P. Wölfle, Rev. Mod. Phys. **79**, 1015 (2007).
[7] D. Belitz, T. R. Kirkpatrick, and T. Vojta, Rev. Mod. Phys. **77**, 579 (2005).
[8] H. J. Williams, J. H. Wernick, R. C. Sherwood, and G. K. Wertheim, J. Appl. Phys. **37**, 1256 (1966).
[9] G. S. Knapp, F. Y. Fradin, and H. V. Culbert, J. Appl. Phys. **42**, 1341 (1971).
[10] B. T. Matthias, A. M. Clogston, H. J. Williams, E. Corenzwit, and R. C. Sherwood, Phys. Rev. Lett. **7**, 7 (1961).
[11] W. E. Gardner, T. F. Smith, B. W. Howlett, C. W. Chu, and A. Sweedler, Phys. Rev. **166**, 577 (1968).
[12] J. H. Fluitman, B. R. de Vries, R. Boom, and C. J. Schinkel, Phys. Lett. A **28**, 506 (1969).
[13] J. Mathon, Proc. R. Soc. London A **306**, 355 (1968).
[14] U. Zülicke and A. J. Millis, Phys. Rev. B **51**, 8996 (1995).
[15] A. J. Millis, Phys. Rev. B **48**, 7183 (1993).
[16] M. Nicklas, M. Brando, G. Knebel, F. Mayr, W. Trinkl, and A. Loidl, Phys. Rev. Lett. **82**, 4268 (1999).
[17] P. G. Niklowitz, F. Beckers, G. G. Lonzarich, G. Knebel, B. Salce, J. Thomasson, N. Bernhoeft, D. Braithwaite, and J. Flouquet, Phys. Rev. B **72**, 024424 (2005).
[18] D. A. Sokolov, M. C. Aronson, W. Gannon, and Z. Fisk, Phys. Rev. Lett. **96**, 116404 (2006).

[19]F. M. Grosche, C. Pfleiderer, G. J. McMullen, G. G. Lonzarich, and N. R. Bernhoeft, Physica B **206-207**, 20 (1995).
[20]C. Pfleiderer, G. J. McMullan, S. R. Julian, and G. G. Lonzarich, Phys. Rev. B **55**, 8330 (1997).
[21]M. Uhlarz, C. Pfleiderer, and S. M. Hayden, Phys. Rev. Lett. **93**, 256404 (2004).
[22]C. Pfleiderer, S. R. Julian, and G. G. Lonzarich, Nature (London) **414**, 427 (2001).
[23]N. Doiron-Leyraud, I. R. Walker, L. Taillefer, M. J. Steiner, S. R. Julian, and G. G. Lonzarich, Nature (London) **425**, 595 (2003).
[24]S. S. Saxena, P. Agarwal, K. Ahilan, F. M. Grosche, R. K. W. Haselwimmer, M. J. Steiner, E. Pugh, I. R. Walker, S. R. Julian, P. Monthoux, G. G. Lonzarich, A. Huxley, I. Sheikin, D. Braithwaite, and J. Floquet, Nature (London) **406**, 587 (2000).
[25]D. Aoki, A. Huxley, E. Ressouche, D. Braithwaite, J. Floquet, J.-P. Brison, E. Lhotel, and C. Paulsen, Nature (London) **413**, 613 (2001).
[26]T. Akazawa, H. Hidaka, H. Kotegawa, T. C. Kobayashi, T. Fujiwara, E. Yamamoto, Y. Haga, R. Settai, and Y. Onuki, Physica B **359–361**, 1138 (2005).
[27]N. T. Huy, A. Gasparini, D. E. de Nijs, Y. Huang, J. C. P. Klaasse, T. Gortenmulder, A. de Visser, A. Hamann, T. Gorlach, and H. v. Löhneysen, Phys. Rev. Lett. **99**, 067006 (2007).
[28]D. Fay and J. Appel, Phys. Rev. B **22**, 3173 (1980).
[29]K. B. Blagoev, J. R. Engelbrecht, and K. S. Bedel, Phys. Rev. Lett. **82**, 133 (1999).
[30]Z. Wang, W. Mao, and K. S. Bedell, Phys. Rev. Lett. **87**, 257001 (2001).
[31]R. Roussev and A. J. Millis, Phys. Rev. B **63**, 140504 (2001).
[32]D. Belitz and T. R. Kirkpatrick, Phys. Rev. B **69**, 184502 (2004).
[33]A. V. Chubukov, A. M. Finkel'stein, R. Haslinger, and D. K. Morr, Phys. Rev. Lett. **90**, 077002 (2003).
[34]V. Y. Markiv and N. N. Balyavina, Dopov. Akad. Nauk. Ukr. RSR (Ser. A) **6**, 70 (1987).
[35]V. Keppens, D. Mandrus, B. C. Sales, B. C. Chakoumakos, P. Dai, R. Coldea, M. B. Maple, D. A. Gajewski, E. J. Freeman, and S. Bennington, Nature (London) **395**, 876 (1998).
[36]M. Seeger, S. N. Kaul, H. Krönmuller, and R. Reisser, Phys. Rev. B **51**, 12585 (1995).
[37]Y. Kats, L. Klein, J. W. Reiner, T. H. Geballe, M. R. Beasley, and A. Kapitulnik, Phys. Rev. B **63**, 054435 (2001).
[38]A. Semwal and S. N. Kaul, Phys. Rev. B **64**, 014417 (2001).
[39]S. Süllow, I. Prasad, M. C. Aronson, S. Bogdanovich, J. L. Sarrao, and Z. Fisk, Phys. Rev. B **62**, 11626 (2000).
[40]M. Seeger and H. Kronmüller, J. Magn. Magn. Mater. **78**, 393 (1989).
[41]N. P. Butch and M. B. Maple, Phys. Rev. Lett. **103**, 076404 (2009).
[42]J. C. Le Guillou and J. Zinn-Justin, Phys. Rev. Lett. **39**, 95 (1977).
[43]M. Campostrini, A. Pelissetto, P. Rossi, and E. Vicari, Phys. Rev. E **60**, 3526 (1999).
[44]C. Holm and W. Janke, Phys. Rev. B **48**, 936 (1993).
[45]P. R. Rhodes and E. P. Wohlfarth, Proc. R. Soc. London **273**, 247 (1963).
[46]J. H. Wernick, G. K. Wertheim, and R. C. Sherwood, Mater. Res. Bull. **7**, 1431 (1972).
[47]S. M. Stishov, A. E. Petrova, S. Khasanov, G. Kh. Panova, A. A. Shikov, J. C. Lashley, D. Wu, and T. A. Lograsso, J. Phys. Condens. Matter **20**, 235222 (2008).
[48]C. Pfleiderer, A. Faißt, H. von Lohneysen, S. M. Hayden, and G. G. Lonzarich, J. Magn. Magn. Mater. **226–230**, 258 (2001).
[49]S. J. C. Yates, G. Santi, S. M. Hayden, P. J. Meeson, and S. B. Dugdale, Phys. Rev. Lett. **90**, 057003 (2003).
[50]L. Taillefer, G. G. Lonzarich, and P. Strange, J. Magn. Magn. Mater. **54–57**, 957 (1986).
[51]R. P. Smith, M. Sutherland, G. G. Lonzarich, S. S. Saxena, N. Kimura, S. Takashima, M. Nohara, and H. Takagi, Nature (London) **455**, 1220 (2008).
[52]Y. Aoki, T. Namkik, S. Ohsaki, S. R. Saha, H. Sugawara, and H. Sato, J. Phys. Soc. Jpn. **71**, 2098 (2002).
[53]F. R. de Boer, C. J. Schinkel, J. Biesterbos, and S. Proost, J. Appl. Phys. **40**, 1049 (1969).
[54]E. D. Bauer, A. D. Christianson, J. S. Gardner, V. A. Sidorov, J. D. Thompson, J. L. Sarrao, and M. F. Hundley, Phys. Rev. B **74**, 155118 (2006).
[55]E. D. Bauer, V. S. Zapf, P.-C. Ho, N. P. Butch, E. J. Freeman, C. Sirvent, and M. B. Maple, Phys. Rev. Lett. **94**, 046401 (2005).